Free-surface RANSE simulations for steady and unsteady ship flows

Rodrigo Azcueta, MTG Marinetechnik GmbH[1]

1 INTRODUCTION: In this work the RANSE solver COMET was extended to both include the ship's running attitude in the calculations, and to simulate the motions of ships floating at the free surface. The work was presented as a PhD thesis, (*Azcueta* (2001), pdf file can be sent on request). This paper is a brief summary of it. RANSE computations are increasingly being used to predict the ship resistance. In recent years the deformation of the free-surface and hence the wave-making resistance have been successfully implemented and validated. But to date the ship's running attitude, i.e. the dynamic sinkage and trim of the ship underway, has been neglected, even in research applications. All viscous flow computations known to me are to date in the *model-fixed* condition, either at the floating attitude at rest or at the running attitude measured in the towing tank. To improve the resistance predictions further, the ship's running attitude has to be included in the computations (*model-free* condition), since its effect is usually significant. This was the first aim of this work. The second was to extend the numerical method to simulate the motions of bodies floating freely at the free surface in the 6 DOF. An important requirement was to implement the coupling of the body motions and the fluid flow in such a way that both types of simulations – steady and unsteady – could be performed with the same program, and that the method be extensible to still more complex tasks, such as for ship manoeuvring and ships in waves.

2 NUMERICAL METHOD: The flow solver used is based on a Finite Volume Method with unstructured meshes and an *interface-capturing scheme* to determine the shape of the free surface, *COMET* (2000). The method was extended with an *user-programmed rigid-body* module to couple the body motions in the 6 DOF with the fluid flow. A *single-grid* strategy was used, where a rigid, body-fixed grid moves relative to an inertial frame of reference and the ficticious flow forces are automatically taken into account in the flow equations. The rigid body module is linked and run simultaneously with the flow solver and can thus operate and update all flow variables, boundary conditions and parameters of the numerical method.

3 EXTRAPOLATION TO GRID-INDEPENDENT SOLUTION: Prior to extending the method to simulate body motions, the RANSE solver was extensively tested to assess the accuracy of the resistance prediction. Turbulence modelling, time integration, and the discretisation scheme used for the momentum equations were systematically investigated, see *Azcueta* (2001) for details. Here, only the latter aspect will be briefly addressed. Blending central-differencing (CDS) with upwind-differencing (UDS) is a widely used method to obtain an accurate flow prediction free from oscillations. However, for each discretisation scheme resulting from the different UDS/CDS ratios, the computed pressure distribution changes substantially. Figure 1 shows the behaviour of C_P for three systematically refined grids as an idealised sketch and Figure 2 for a real flow around a submerged hydrofoil. The strong dependency of C_P on the UDS-CDS ratio has been made used of to propose an alternative extrapolation method to the well known *Richardson extrapolation*, which attains the same accuracy computing only on the first two coarse grids. The grid-independent solution is found at the intersection of the two (basically straight) lines from the coarse and medium grid results. The time saving for not computing on the finest grid is at least a factor 10.

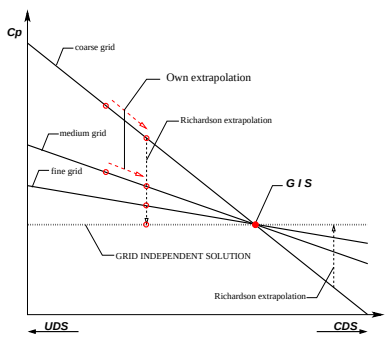

Figure 1: Idealised dependence of C_p on UDS-CDS ratio.

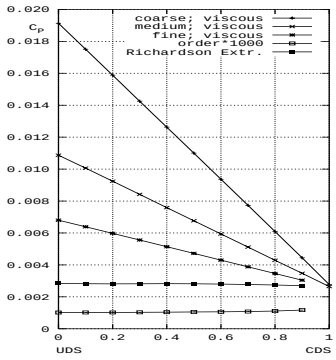

Figure 2: Dependence of C_p on UDS-CDS ratio for a real case.

[1]Wandsbeker Königstr. 62, D-22041 Hamburg, Azcueta@MTG-Marinetechnik.de

4 SHIP'S RUNNING ATTITUDE

Series 60 Hull: Calculations at $F_n = 0.316$ for the straight-ahead condition and for the smallest measured drift angle ($\beta = 2.5\,^\circ$) were performed and compared with measurements from the University of IOWA by *Longo and Stern* (1996). A coarse grid with $38{,}912$ CVs was used. In the following, only the 0°–drift case will be presented. Table 1 shows the comparison of computed results with experimental data. As shown before, the amount of CDS in UDS influences the computed pressure distribution. The results of the table are for 80% CDS. The computation under-predicts the measured total resistance coefficients by 14.6% in the model-fixed and by 5.9% in the model-free case. Thus, the inclusion of the running attitude in the calculations improves the agreement with the experiments by 10%. The computed wetted surface for the model-free condition grows by 4.7%. The computed sinkage and trim angle under-predict the measurements by about 8% and 6%, respectively. All computed resistance coefficients include the air resistance, which accounts on average for $1.5\% - 2.0\%$ of the total resistance. The CPU-time needed per time step for the model-free calculations increases by about 50% compared to the model-fixed case. The convergence history of forces and motions for the model-free condition is shown in Figure 3. These calculations were performed varying the ratio of UDS-CDS. Until 50 s, pure UDS was used. From there on, UDS was blended with CDS in 10% and 10 s steps. In the diagram, we can clearly see the dependence of the pressure resistance coefficient and the trim angle on the UDS-CDS mixing ratio. At 12.5 s the heave motion was released. The heave force (normalised for 1 m model) increases from 38.3 N to 41.5 N and balances exactly the model displacement. At 25 s the pitch motion was also released. In the converged final position (with 80% CDS) the hull is trimmed $0.1\,^\circ$ by the bow, and the sinkage accounts for 0.36% of L. The trim moment is in balance with the trim moment caused by the towing force. The convergence histories for the 2.5°–drift condition (model also free to heel) show the same behaviour as for the 0°–drift condition. The heel moment and side force also show a strong dependence on the UDS-CDS ratio.

	C_T $[\times 10^{-3}]$	sinkage $[\times L]$	trim $[^\circ]$	S_{wet} $[\times L^2]$
A: exp. (free)	5.96	-0.00392	-0.100	0.1699
B: comp. (fixed)	5.09	0.00000	0.000	0.1701
C: comp. (free)	5.61	-0.00360	-0.094	0.1779
$(B-A)/A$	-14.6%	–	–	0.1%
$(C-A)/A$	-5.9%	-8.2%	-6.0%	$+4.7\%$
$(C-B)/B$	$+10.2\%$	–	–	$+4.6\%$

Table 1: Comparison of measured and calculated values ($0\,^\circ$–drift condition)

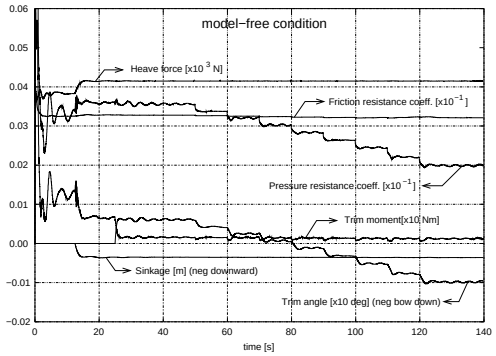

Figure 3: Convergence history (model-free)

Blunt-Bow Ship Model (Breaking Waves): The next computations are for the model of a very fat ship with a blunt bow. In this case the emphasis was on the large change in running attitude and thus resistance, as well as on the bow-wave breaking pattern and its comparison with model tests from the Ship Research Institute in Tokyo. Figure 4 shows a sketch of the used model. The Froude number based on the hull draft was $F_n = 0.7$ and the Reynolds number around $3.4 \cdot 10^6$. Three grids with substantially different fineness in the free-surface region (up to $2{,}147{,}628$ CVs) were used in order to assess the grid-dependence of the computed wave patterns. Figure 5 shows the average position of the model and the contour of the free surface for the *model-fixed, sinkage-only* and *model-free* conditions. While the wave profile does not

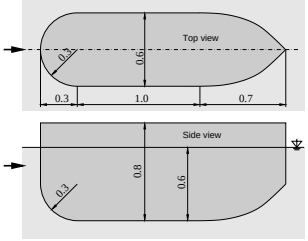

Figure 4: Sketch of the used model.

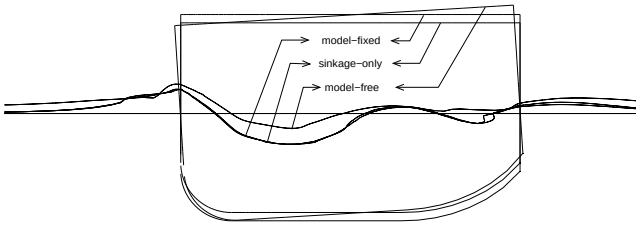

Figure 5: Model position and wave profile for the model-fixed, sinkage-only and model-free conditions.

change much for the sinkage-only condition, it looks quite different for the final trimmed attitude. The difference in free-surface shape is associated with large changes in force coefficients. The wetted surface underway increases by about 9%, the total resistance coefficient by 26%, mostly due to the predominant C_P values. Unfortunately, only measurements for the sinkage-only condition were available for validation. The computed resistance and sinkage were predicted with an accuracy of 6% and 9%, respectively. The agreement is thus quite satisfactory.

5 FREELY-FLOATING BODIES

In addition to the computation of the ship's running attitude (steady-state flow), simulations of the unsteady response of bodies released from a position out of equilibrium were performed.

Drop Tests (Plane Motion): The first example are simulations of 2-D drop tests with a prismatic wedge of $20\,^\circ$ deadrise and a high aspect ratio (0.61 m $\times$ 2.44 m). Such drop tests are of relevance for investigating slamming problems. This test case was useful to validate the method with existing experimental data from *Peterson et al.* (1997). For an accurate simulation of water-entry phenomena and the associated ship responses and slamming forces, strong deformation of the free surface including jets, sprays, splashing, air trapping, and breaking waves have to be considered. The free-surface feature of the flow solver COMET has proven to be well suited for this task, *Azcueta et al.* (1999). In the present simulations the body trajectory, velocity and forces (in the planar 3-DOF) are obtained from the flow forces acting on the body, starting from the initial condition, without the need for prescribing the body motion. Unlike the experimental drop tests, the simulations do not only yield the vertical and angular accelerations, but also the transverse acceleration, as well as the water impact forces at each point of the model as a function of time. The physical model was dropped from different heights, with different weights, and with initial zero or non-zero heel angles. The numerical mesh used was relatively coarse with less than $15{,}000$ CVs. It extended 2 m to the sides, 1 m from the keel upwards, and 1.5 m from the keel downwards. The drop height was 0.61 m. Figure 6 compares the simulated vertical and angular acceleration, vertical or impact velocity and angle of heel for an asymmetric drop tests ($5\,^\circ$ heel) in the medium-weight condition ($W = 293$ kg, $I_{xx} = 10.95$ kgm^2), with the corresponding experimental data. The experimental results contain mechanical vibrations associated with structural resonances, making a precise quantitative comparison between simulation and experiment difficult. Nevertheless, the comparison shows a surprisingly good agreement both for the magnitude and timing of the maximum accelerations and velocities.

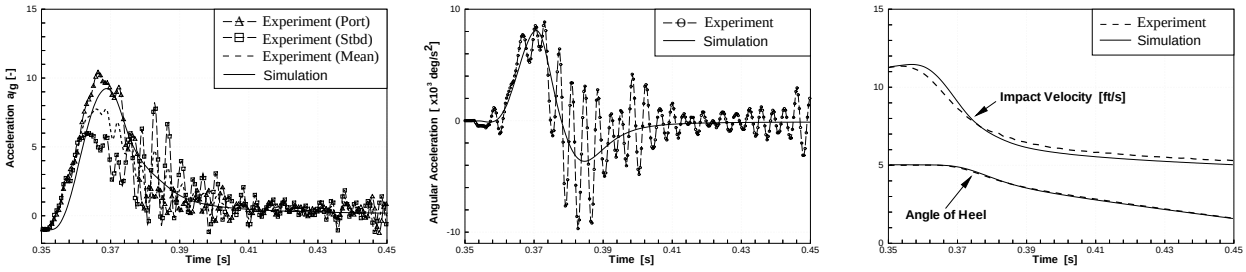

Figure 6: Comparison of measured and simulated results for an asymmetric drop test.

Boat Section (Plane Motion): The next application case is a roll extinction test (roll, heave and sway) with the midship section of a sailing boat with and without the keel. With these simulations the differences in roll damping due to the keel were quantified. Furthermore, the robustness of the numerical method for simulating large amplitude motions was addressed. The boat is a modern sailing yacht of 10 m length and 3 m beam (Dehler 33'). The numerical mesh was relatively coarse with $5{,}192$ CVs. It was extended by a block above deck to allow large roll angles. Figure 7 on the left shows one half of the computational domain and on the right a close-up view of the hull/keel region. To induce a roll motion, the boat was initially inclined $30\,^\circ$ in calm water to one side, and then suddenly let to roll freely. Figure 8 shows the time history of sway, heave and roll motion for the simulations with and without the keel for the first roll periods. The section without the keel completes the first period in 2.9 s and the roll angle decreases by 6.4° in this period of time, while the section with the keel needs 4.3 s to reduce the roll angle by 18.8°. The logarithmic decrement together with the roll period were calculated for both cases. They characterise the roll damping coefficient. They are much larger for the case with the keel ($\delta_{keel} = 2.9$ to $\delta_{no-keel} = 4.2$). Another big difference

induced by the keel is in the sway response. As the hull section rights up, the keel acts like a lever pushing the hull to the left side (dotted line in the negative area in Figure 8). Without the keel the hull presses the water to the left, and gets an impulse to the right (dotted line in the positive area).

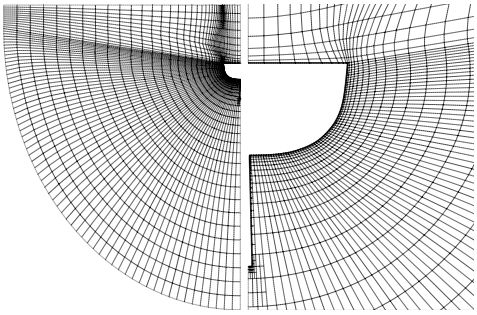

Figure 7: Numerical mesh.

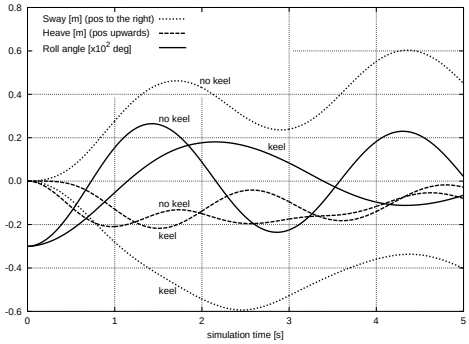

Figure 8: Time history of motions.

Sailing Boat in Planing Condition (3-D Case): The last application case is the 3-D coupled roll, pitch, sway and heave motion of the sailing boat of the example above at full speed ($v_b = 7$ m/s; $F_n = 0.7$, bare hull). The aim of this application was to show how both steady-state and transient problems can be simulated with the same computer program by simply adjusting the appropriate parameters of the numerical method. These simulations are performed for the full scale boat using the standard k-ϵ turbulence model with wall functions ($R_n = 7 \cdot 10^7$). The numerical mesh had a total of $280{,}000$ CVs. Figure 9 shows the time history of the motions for the computation optimised to converge to the steady-state final sailing attitude. Figure 10 is for the time-accurate simulation of the boat motions. The boat was initially constrained in an inclined position ($15\,^\circ$) until the steady-state flow was reached. Then the 4 DOF were released simultaneously. The pitch angle converges to about $5\,^\circ$. While in the first case the roll angle directly converges to near cero, in the real motion it takes many roll periods. Without the keel and rudder, the roll motion is slightly damped, but due to the forward speed more than in the 2-D case without the appendages. Due to the lack of experiments, this simulation could not be validated so far.

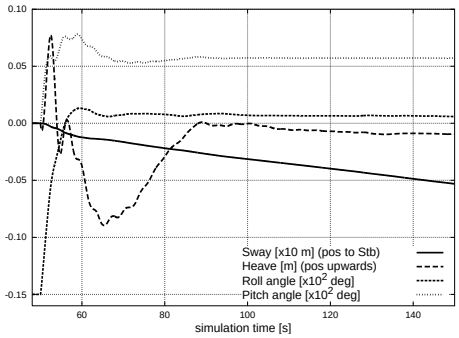

Figure 9: Motion history accelerated for convergence to steady-state sailing attitude.

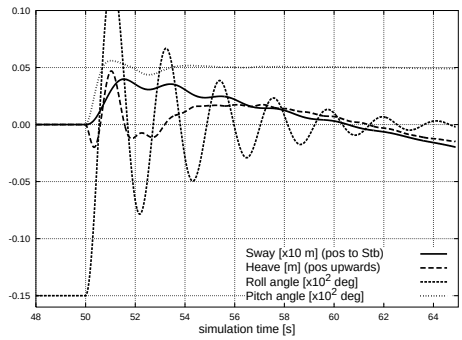

Figure 10: Motion history of the transient motion.

6 REFERENCES

Azcueta, R., 2001. *Computation of Turbulent Free-Surface Flows Around Ships and Floating Bodies.* PhD. thesis, Technical University Hamburg-Harburg (pdf file on request at rodrigo@azcueta.de).

Azcueta, R., Muzaferija, S., and Perić, M., *Computation of Breaking Bow Waves For A Very Fat Hull Ship*,7th International Conference on Numerical Ship Hydrodynamics, Nantes, 1999.

COMET, *Version 2.000 – User Manual*, ICCM GmbH, 2000.

Longo, J. and Stern, F., *Yaw Effects on Model-Scale Ship Flows*, Proceedings of the 21st Symposium on Naval Hydrodynamics, Trondheim, 1996.

Peterson, R. and Wyman, D. and Frank, C., 1997, *Drop tests to support water-impact and planing boat dynamics theory*, CSS Technical Report, Coastal Systems Station, Panama City.

7 *References

Azcueta, R., 2001. *Computation of Turbulent Free-Surface Flows Around Ships and Floating Bodies*. Ph.D. thesis, Technische Universität Hamburg-Harburg.

Azcueta, R., Muzaferija, S., and Perić, M., *Computation of breaking bow waves for a very fat hull ship*. In *7th International Conference on Numerical Ship Hydrodynamics*. Nantes, 1999.

COMET, *Version 2.000 – User Manual*. ICCM Institute of Computational Continuum Mechanics GmbH, 2000.

Longo, J. and Stern, F., *Yaw effects on model-scale ship flows*. In *Proceedings of the 21st Symposium on Naval Hydrodynamics*. Trondheim, Norway, 1996.

Peterson, R., Wyman, D., and Frank, C., 1997. *Drop tests to support water-impact and planing boat dynamics theory*. *CSS technical report*, Coastal Systems Station, Panama City, USA. TR-97.